UDC 621 . 746 . 27 : 536 . 55

Technical Report

Electromagnetic Sensor Just below Continuous Casting Mold by Using Magnetic Transformation of Steel

Hiroshi HARADA*
Tomohiro KONNO
Takehiko TOH
Masaki NAGASHIMA
Masanori YAMANA

Abstract

We propose an electromagnetic sensor to measure the slab surface temperature of the narrow face by using the magnetic transformation just below the CC mold, taking into account that the narrow face of the slab has been cooled below the Curie temperature beneath the mold. The principle of the proposed sensor is that the imposed magnetic field on the slab surface is governed by the electromagnetism of the slab surface, in other words, the slab surface temperature and induced electric voltage due to the change of the imposed magnetic field are measured to estimate the slab surface temperature by using the relationship between electric voltage and surface temperature. As preliminary experiments, laboratory experiments have been performed to clarify the relationship between the temperature and induced electric voltage, when the AC magnetic field has been imposed on the slab surface. Moreover, plant tests have been conducted by installing the sensor just below the narrow face of the mold to show that the proposed sensor could measure surface temperature under severe conditions and comprehensively evaluate the fluid flow and solidification behavior in the CC mold.

1. Introduction

The molten steel flow in the mold greatly affects casting stability and slab quality. In **Fig. 1**, when the molten steel poured into the mold deviates and impinges on the solidified shell, the solidified shell remelts. When its remelting becomes pronounced, the solidified shell is thinned locally. This lack of shell growth might cause shell bulging just below the narrow face rolls and lead to an operational problem called a breakout. In addition, the deviated flow increases the downward flow velocity in the CC strand, the occurrence of bubble-related internal defects, and the meniscus inversion flow velocity. These conditions in turn may cause mold powder entrapment and other defects. This makes it necessary to properly control the nozzle discharged flow and to suppress the buildup of nonmetallic inclusions in the submerged entry nozzle. It is also necessary to detect deviated flow and to prevent slab defects and casting problems by optimizing casting conditions. Among general deviated flow detection techniques, one method is that a predetermined pro-

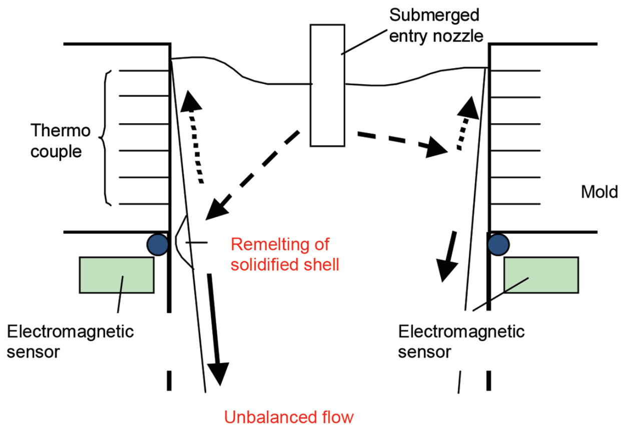

Fig. 1 Schematic view of unbalanced flow in continuous casting strand

* Chief Researcher, Doctor of Engineering, Casting-Rolling Research Lab., Process Research Laboratories
20-1 Shintomi, Futtsu City, Chiba Pref. 293-8511

portion of the peak temperatures measured with thermocouples embedded in the narrow face copper plates of the mold locates the meniscus position and the difference in the peak temperatures between both narrow faces is evaluated as the deviated flow index.[1)] Another method measures the inlet and outlet water temperatures and inlet water flow rate of the narrow face copper plates, determines the heat fluxes from the measured values, and takes the difference in the heat fluxes between both narrow faces as the deviated flow index.[1, 2)] However, it is difficult for either method to detect the deviated flow in the strand.

A better method for detecting deviated flow in the strand is described now. When deviated flow occurs, it produces differences in shell remelting or shell growth rate and changes the slab temperature between both narrow faces. Also, intense cooling just below the mold narrow faces magnetically transforms the slab surface. Given these facts, we studied an electromagnetic sensor capable of stably measuring the slab surface temperature in a high-temperature water vapor atmosphere just below the mold.[3–5)]

2. Principle of Electromagnetic Sensor and Verification of Principle by Laboratory Experiment

With continuous slab casting, the strand is supported on the broad faces with many rolls from just below the mold to near the final solidification position. On the narrow faces, the strand is supported only with a few rolls provided just below the mold. For this reason, cooling of the narrow faces of the slab must rely on cooling from the broad faces. Generally, therefore, the slab is intensely cooled just below the mold. The slab surface temperature pattern thus becomes as schematically shown in **Fig. 2**. What should be noted here is that the slab surface temperature Ts drops to the Curie temperature Tc and then rises up due to reheating. The Curie temperature is the magnetic transformation temperature. Steel changes from ferromagnetic to paramagnetic at the Curie temperature and then to nonmagnetic at higher temperatures.

When an AC magnetic field is applied to the slab surface as shown in **Fig. 3** and the slab surface temperature is much higher than the Curie temperature, the applied magnetic field penetrates as in a vacuum and expands in the slab as indicated by the broken lines in Fig. 3. When the slab surface is magnetized, the magnetic field is concentrated in the magnetized region as indicated by the solid lines in Fig. 3. The magnetic field lines are greatly changed as a result. This magnetic field line change depends on the slab surface temperature or slab surface magnetism. For this reason, the magnetic field line change is detected with separately installed coils and the slab surface temperature is determined by using a separately defined equation relating the induced electromotive force to the slab surface temperature.

Figure 4 shows the system configuration of an electromagnetic sensor. The electromagnetic sensor consists of a solenoid-shaped primary coil and a secondary coil. The secondary coil is installed at the front of the primary coil. The coils were housed in a stainless steel-made cylindrical case. The inside of the cylindrical case was force-cooled with dry air. The primary coil was energized by a low-frequency AC current through a constant-current amplifier and applied the AC magnetic field vertical to the slab surface. The voltage signals of the secondary coil were denoised through a low-path filter. The same frequency components as those of the primary current were detected by using a lock-in amplifier.

A laboratory experiment was conducted to verify the principle of the proposed electromagnetic sensor. Specifically, a slab sample was

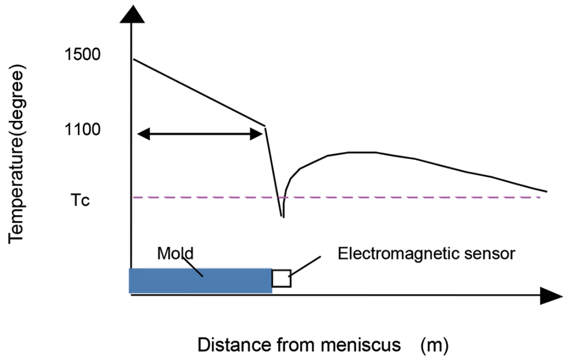

Fig. 2 Schematic view of slab surface temperature profile at narrow face during casting

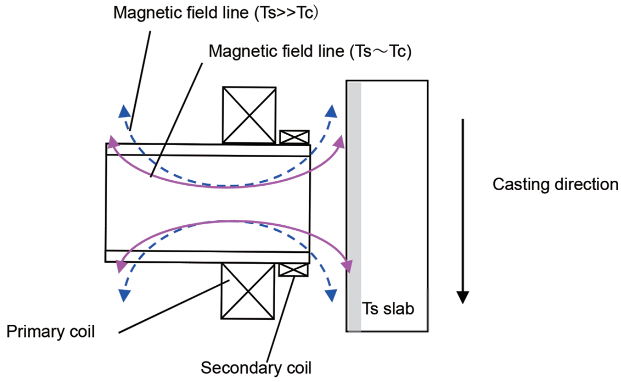

Fig. 3 Schematic view of the proposed electromagnetic sensor and the change of magnetic field line due to slab surface temperature

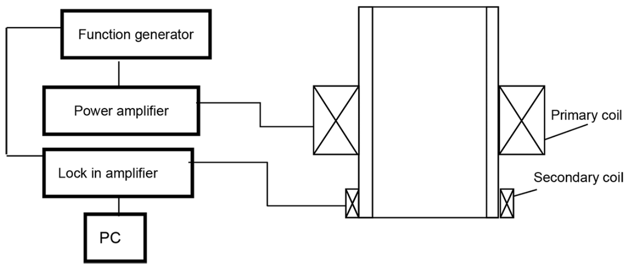

Fig. 4 Measurement system of electromagnetic sensor

charged into a reheating furnace, heated to 1300°C, and removed from the reheating furnace. The above-mentioned electromagnetic sensor was placed above the heated slab sample. A thermocouple was set at about 1 mm below the surface of the slab sample. The temperature of the slab sample and the voltage of the secondary coil were measured. The results measured with the sensor placed at 30 mm above the slab are shown in **Fig. 5** as an example of the measured results. The voltage measured with the secondary coil is almost constant at temperatures below the Curie temperature and at higher temperatures, but changes in the range marked by the double-ended arrow in Fig. 5. The voltage-slab surface temperature relationship in the double-ended arrow marked range was obtained by polynomial approximation as shown in **Fig. 6**. The experimental results can be reproduced by cubic equations (1) and (2). In the plant test described in the next section, the slab surface temperature was

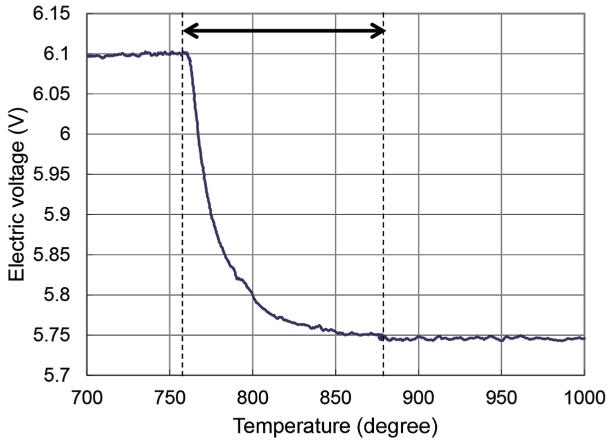

Fig. 5 Relationship between slab surface temperature and induced electric voltage of secondary coil

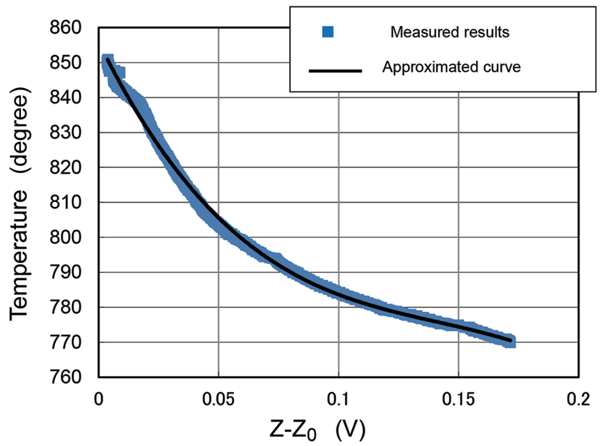

Fig. 6 Approximated curve about the relationship between induced electric potential of secondary coil and surface temperature

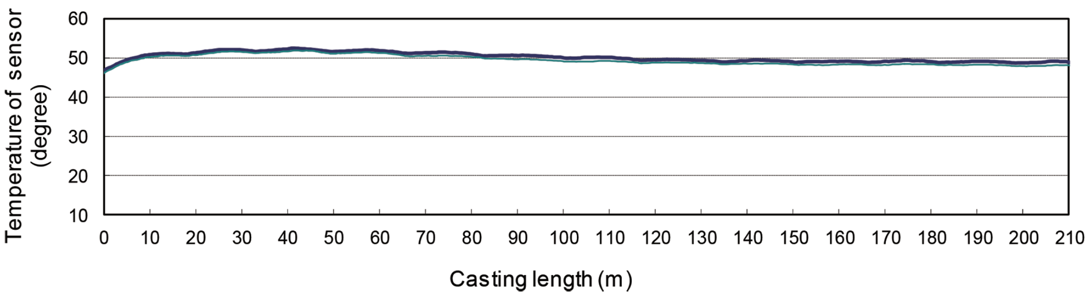

Fig. 7 Successive change of sensor temperature during casting

estimated from the measured voltage results by using Equations (1) and (2).

$$V = Z - Z_0 \quad (1)$$

$$T = -20065V^3 + 8752.8V^2 - 1390.8V + 858.8 \quad (2)$$

$$R^2 = 0.9967 \quad (3)$$

where T is temperature (degree), Z is voltage (V), and Z_0 is secondary coil voltage (V) in the nonmagnetic region.

3. Results Measured with Electromagnetic Sensor in Plant Test and Discussion

The above-mentioned electromagnetic sensor was installed just below the narrow face mold. The electromagnetic sensor was placed in the stainless steel-made cylindrical container and its inside was constructed for air cooling. Since the electromagnetic sensor is directly installed below the mold narrow faces, its distance to the slab can be held constant even when the slab width is changed. However, the installation of the electromagnetic sensor just below the mold narrow faces may cause temperature drift due to the radiant heat of the slab. Thereupon, a thermocouple is installed in the electromagnetic sensor to investigate the temperature change of the electromagnetic sensor during casting. An example of the measured results is shown in **Fig. 7**. It is evident that the temperature rise of the electromagnetic sensor is slight during casting. This is because part of the secondary cooling water was constantly applied onto the electromagnetic sensor. Consequently, the electromagnetic sensor could stably measure the slab temperature while the mold with the electromagnetic sensor was installed on the continuous caster.

Plant tests were performed under the conditions shown in **Table 1** and the obtained electromagnetic sensor signals were analyzed.

Table 1 Casting conditions of plant test

Slab width	1000–1800 mm
Casting speed	0.75–1.2 m/min
Steel grade	Middle carbon Al-killed steel, low carbon Al-killed steel
Sensor position	(i) Vertical position: just below the narrow face of mold (ii) Distance between sensor and narrow face of slab: 30 mm

First, a test was conducted to change the secondary cooling water spray rate on the narrow face side. The results are shown in **Fig. 8**. High voltage corresponds to low slab surface temperature and vice versa. The voltage of the electromagnetic sensor is seen to rapidly change with the change in the secondary cooling water flow density. This means that the slab surface temperature rapidly changes with the spray water flow rate. The secondary coil voltage of the electromagnetic sensor changes with the slab surface temperature or the slab surface magnetic property.

In Fig. 8, the secondary cooling water flow rate is the same at 14500 s and 16000 s. The electromagnetic sensor voltage is approximately the same at 14500 s and 16000 s. These results confirm that the reproducibility of the electromagnetic sensor is high. Another experiment was conducted to change the cooling water flow rate during casting and to investigate the relationship between the secondary cooling water flow density and the slab surface temperature.

The slab surface temperature shown along the vertical axis of **Fig. 9** is converted from the surface temperature by using the relationship shown in Fig. 6. It is also confirmed from Fig. 9 that a good relationship is observed between the narrow face cooling water flow rate and the slab surface temperature.

Next, a pair of the aforementioned electromagnetic sensors has been installed just below both narrow faces of the mold to measure the slab surface temperature continuously. The change in the slab surface temperature during a cast as well as the slab surface temperature deviation between both narrow faces can be evaluated by plotting the slab surface temperature of one narrow face (narrow face B) along the vertical axis and the slab surface temperature of the other narrow face (narrow face A) along the horizontal axis. An example of stable casting throughout a cast is shown in **Fig. 10** as a typical example of the measured results. As the casting speed and the casting width changes during the cast, the average slab surface temperature changes. The slab surface temperatures on both narrow faces as estimated with the electromagnetic sensors are distributed from the bottom left corner to the top right corner of Fig. 10. Also, the slab surface temperature scatter is large when the slab surface temperatures are high. Despite some scatter during the cast, the slab temperatures converted from the signals of both electromagnetic sensors are plotted centered around the y=x line and are not deviated to either side.

Figure 11 shows an example in which nozzle clogging proceeded with the progress of casting. In Fig. 11, the slab surface temperatures are plotted in two parts: (a) data in the first half of the cast without nozzle clogging and (b) data in the last half of the cast with notable nozzle clogging. The slab surface temperatures are concentrated in the bottom left corner of Fig. 11 in the first half of the cast without nozzle clogging and are greatly scattered in the last half of the cast with conspicuous nozzle clogging. The temperature differences between both narrow faces are larger in the last half of the cast. When the slab surface temperatures in the first half of the cast in Fig. 11 are compared with those in Fig. 10, it is evident that the slab surface temperatures on narrow face B are lower than those on narrow face A in the first half of the cast in Fig. 11. From Figs. 10 and 11, it is clear that the nozzle discharged flow greatly affects the solidified shell growth and that the deviation of the nozzle discharged flow creates the differences in the solidified shell growth and consequently in the slab surface temperatures.

As described above, the variation of the slab surface temperature with steel types and casting conditions can be detected by using electromagnetic sensors that make use of the magnetic transformation just below the mold narrow faces. In addition, the flow of the molten steel in the mold and the solidified shell growth can be com-

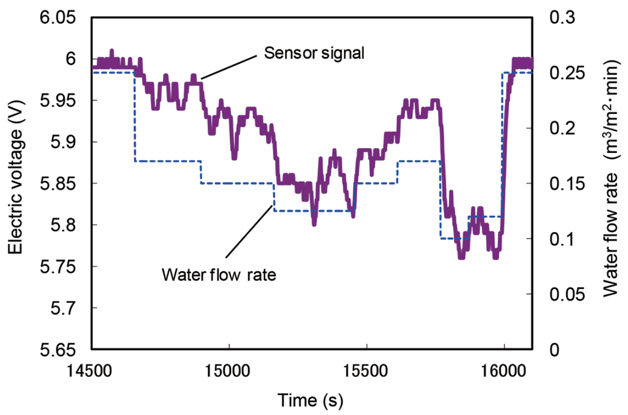

Fig. 8 Successive change of sensor signals in the condition which water flow rate of spray at narrow face changes

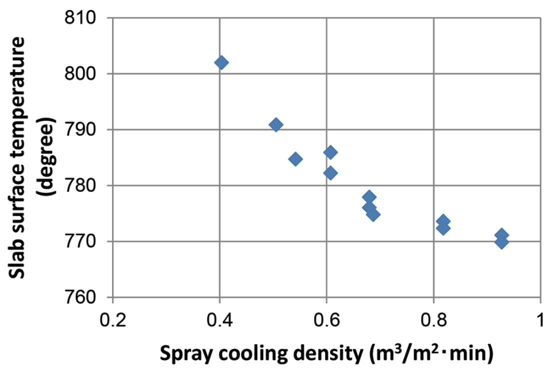

Fig. 9 Effect of water flow rate of spray at narrow face on the estimated slab surface temperature

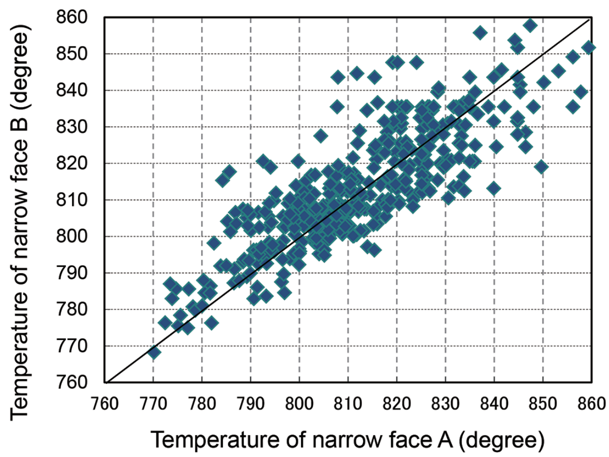

Fig. 10 Successive change of surface temperature at both narrow faces in the sequential casting

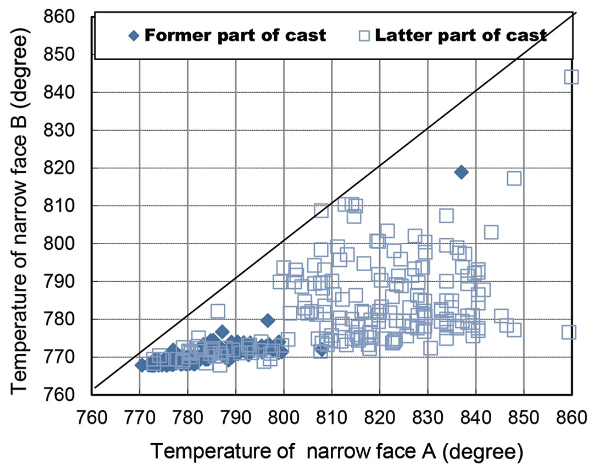

Fig. 11 Successive change of surface temperature at both narrow faces in the sequential casting
(Cast data with occurrence of nozzle clogging are plotted.)

prehensively diagnosed by installing electromagnetic sensors in both narrow faces of the mold and evaluating the deviations between the electromagnetic sensors.

4. Conclusions

We focused on the magnetic transformation that occurs with the thermal history of the slab just below the mold narrow faces and studied electromagnetic sensors that electromagnetically measure the slab surface temperature. The obtained results are summarized as follows:

(1) By utilizing the fact that the magnetic field lines applied to the slab surface change with the magnetism of the slab surface or with the slab surface temperature, the change of the magnetic lines can be detected as induced electromotive force. The slab surface temperature can be estimated by using an equation relating the induced electromotive force to the slab surface temperature.

(2) The change of the slab surface temperature with the secondary cooling water flow rate can be measured by using the electromagnetic sensors. The variation of the slab surface temperature increases with the progress of nozzle clogging.

(3) The flow of the molten steel in the mold and the solidification of the molten steel can be comprehensively diagnosed by installing electromagnetic sensors just below the mold narrow faces and evaluating the difference in the slab surface temperature between both narrow faces.

References

1) Ohji, M.: 153rd · 154th Nishiyama Memorial Lecture. Tokyo, 1994, ISIJ, p. 1
2) Ishii, T., Tanaka, M., Uehara, A., Kimura, H., Tsutsumi, N.: Proc. Int. Symposium on Electromagnetic Processing of Materials, Nagoya, 1994, ISIJ, p. 396
3) Harada, H., Toh, T., Nagashima, M., Yamana, M.: CAMP-ISIJ. 28, 586 (2015)
4) Harada, H., Toh, T., Nagashima, M., Yamana, M.: CAMP-ISIJ. 29, 650 (2016)
5) Harada, H., Nagashima, M., Toh, T.: Proc. of 8th Int. Symposium on Electromagnetic Processing of Materials, Canne, 2015

Hiroshi HARADA
Chief Researcher, Doctor of Engineering
Casting-Rolling Research Lab.
Process Research Laboratories
20-1 Shintomi, Futtsu City, Chiba Pref. 293-8511

Masaki NAGASHIMA
Senior Manager
Integrated Process Management Dept.
Administration & Planning Div.

Tomohiro KONNO
General Manager, Head of Dept.
Steelmaking Technical Dept.
Steelmaking Div.
Setouchi Works

Masanori YAMANA
General Affairs Division
Hirohata Unit
Nippon Steel Technology Co., Ltd.

Takehiko TOH
Doctor of Environmental Studies
General Manager, Head of Div.
Resource and Process Solition Div.
Nippon Steel Technology Co., Ltd.